Surface evolution of InP substrates at the frontier between deoxidation and dissolution in HCl solutions

Solène Béchu, Damien Aureau, Arnaud Etcheberry

Surface evolution of InP substrates at the frontier between deoxidation and dissolution in HCl solutions

Journal:	*Surface and Interface Analysis*
Manuscript ID	Draft
Wiley - Manuscript type:	Research Article
Date Submitted by the Author:	n/a
Complete List of Authors:	Bechu, Solene; Institut Lavoisier de Versailles, UMR 8180 Aureau, Damien; Institut Lavoisier de Versailles, UMR 8180 ETCHEBERRY, Arnaud; Institut Lavoisier de Versailles, Université de Versailles
Keywords:	XPS, InP, surface evolution

Solène Bechu
Institut Lavoisier de Versailles UMR 8180, CNRS
Université de Versailles Saint-Quentin
45 avenue des Etats-Unis
F-78035 Versailles Cedex, France
Email: solene.bechu@uvsq.fr
Phone: +33 1 39 25 43 96

To:
Editors of Surface and
Interface Analysis

Versailles, 12th, July, 2022

Dear Dr. Abel,

We are pleased to submit our research article entitled "Surface evolution of InP substrates at the frontier between deoxidation and dissolution in HCl solutions" by Solène Béchu, Damien Aureau and Arnaud Etcheberry for publication in the special ECASIA issue of the Surface and Interface Analysis journal.

We confirm that this work is original and has not been published elsewhere nor is currently under consideration for publication elsewhere. In this paper, we explore the surface reactivity of InP substrate when facing different concentrations of HCl. For this purpose, we study by XPS, SEM and AFM the reactivity of (100), (111) and polycrystalline InP substrates when immersed into HCl solutions. We proved that after exceeding a concentration of 6 M, the morphological properties of the InP substrates evolve drastically, with a destructuration of the InP network. However, this destructuration is only morphological since all surfaces conserve a perfect stoichiometry, except the (111) face B, which is initially phosphorus-rich and presents an important release of PH_3 when immersed into HCl 12 M. After the HCl immersion, a small enrichment in indium can be noticed, but with a really low value. This paper highlights the importance of controlling the concentration of HCl during the deoxidation stage, to avoid the morphological destructuration even if the chemical properties are conserved.

We believe that this work is an important tool for the surface and the semiconductor communities regarding the importance of deoxidation for processing semiconductors. Consequently, we think that is of interest to readers in the areas your journal's publications.

In case you accept our manuscript, please note that we are not interested to use the colour versions of our illustrations in the print version.

Please address all correspondence concerning this manuscript to me at solene.bechu@uvsq.fr.

Thank you for your consideration of this manuscript.

Sincerely,

Solène Béchu

Surface evolution of InP substrates at the frontier between deoxidation and dissolution in HCl solutions

Solène Béchu*, Damien Aureau, Arnaud Etcheberry

Institut Lavoisier de Versailles (ILV), Université de Versailles Saint-Quentin-en-Yvelines, Université Paris-Saclay, CNRS, UMR 8180, 45 avenue des Etats-Unis, CEDEX, 78035 Versailles, France

Keywords: X-ray photoemission spectroscopy, InP, surface evolution

Abstract

Surfaces of InP substrates with different crystallographic orientations are investigated when facing HCl solutions. The immersion of (100) InP in a wide range of HCl solutions with different concentrations showed that the frontier between deoxidation and dissolution is around 6 M, with a morphological destructuration. However, no chemical evolutions are noticed even at high concentrations. Similar observations were performed with other crystallographic orientations (polycrystalline and (111) InP substrates), with topographic surface modifications but no chemical ones.

1. Introduction

III-V semiconductors hold a well-established and specific place in the electronic devices industry. Because of the exceptional adaptability of their optical and electrical properties, III-V semiconductors offer the possibility of designing reliable components, targeted as to their use and performing in application fields as diverse as light-emitting diodes, lasers, large wavelength range photodetectors, solar cells, optical switches, quantum well high electron mobility transistors…[1–4]

A strength of III-V materials chemistry is to propose well-defined quaternary, ternary and binary alloys and to combine them by epitaxy in multi-structures, with micrometric or nanometric layers to design energy band diagrams of hetero-structures, with tuneable optical and/or electronical responses for the whole component.[5] The control of these particular objects is achieved by mastering chemical engineering of the interfaces between the layers, the substrate surfaces supporting epitaxy, the final encapsulations, and the etchings. In such a

context, the position of the XPS is obviously a quantitative tool for chemical or even electronic (band-off set) characterizations.

To understand the fundamentals of the III-V chemistry, the researchers have at their disposal binary alloys (InP, InAs, InSb, GaN, GaP, GaAs, GaSb) perfectly mastered. Their comparative study in the face of the same source of interaction is extremely valuable. Here again, XPS plays a central role. Among all III-V binary alloys, InP has a prominent place since it is present in many devices as active device materials, capping layers and even substrates for epitaxial growths, for which surface control is essential.

Indeed, achieving surface chemical controls of InP substrates is a necessity for the growth of high-quality epitaxial films or the device's performance. The key to obtaining such surfaces is the control of intentional oxidation and deoxidation stages. Regarding the deoxidation process, each laboratory possesses its own expertise: thermal desorption of the oxide,[6–8] ion sputtering followed by annealing,[9] H_2 plasma,[10] wet chemical treatments…[11,12] Within the literature, the wet chemical deoxidation of InP is widely described with the importance of the acid choice and how it affects oxide removal.[11,12] HCl is an acid of choice to perform the deoxidation, however, the interactions existing between HCl and InP are very specific, with potential dissolution. Indeed, so lone or in association with other chemicals, HCl concentrated solutions can generate more or less efficient dissolution, governed by an initial interaction between the undissociated HCl molecules and the InP surface lattice. The detailed dissolution mechanisms and associated kinetic rates are available in the literature.[13–17] However if the InP thinning using HCl concentrated solution is established, the chemical surface evolution of InP substrates is barely investigated at high HCl concentrations not saying if, during the dissolution or even the deoxidation processes in HCl, the surface stoichiometry of InP substrates evolves, with a preferential etching of either indium or phosphorus.

This work aims at unveiling the evolution of InP surfaces, either when facing a deoxidation or a dissolution. Indeed, very few works deal with the modifications of InP substrates according to the concentration of HCl solutions or the crystallographic orientations, especially at high concentrations.[18] In order to, XPS, Atomic Force Microscope (AFM) and Secondary Electrons Microscope (SEM) analysis are performed to unveil those evolutions and to understand the mechanisms lying behind.

2. Materials and Methods

2.1. Materials

(100), (111) and polycrystalline n-type InP substrates were purchased from InPact Electronic Materials Ltd. Surfaces were mirror-like finished and denoted as epiready quality by the supplier for the (100) and (111) substrates. Samples were directly immersed for 5 minutes (min) in HCl solutions (37 %, ACS quality, from SUPELCO) at different concentrations (respectively, 3 mol L^{-1} (M), 6 M, 9 M and 12 M). Then, the samples were rinsed for 1 minute in deionised water, dried under N_2 flow and directly transferred within the spectrometer. Air interactions last less than 5 to 10 min.

2.2. XPS

XPS surface chemical analyses were conducted on a Thermo Electron Nexsa spectrometer equipped with a monochromatic Al-Kα X-Ray source (1486.6 eV). The Thermo Electron procedure was used to calibrate the Nexsa spectrometer by using metallic Cu and Au samples intern references (Cu $2p_{3/2}$ at 932.6 eV and Au $4f_{7/2}$ at 84.0 eV). High energy resolution spectra were acquired with an X-ray spot size of 400 µm and using a constant analyzer energy (CAE) mode of 20 eV and 0.1 eV as energy step size. Regarding the nature of the sample, charge compensation wasn't applied. XPS spectra were treated using a Shirley background subtraction, and XPS compositions were deduced using the sensitivity factors and the inelastic mean free paths from Avantage library associated with the spectrometer and the corresponding transmission function.

2.3. SEM

Secondary electron micrographs (SEM) analyses were performed using a JEOL JSM 7001F microscope with a patented "in-lens" Schottky field emission gun (FEG). Imaging analyses were realized at 15 kV accelerating voltage and 10 mm working distance.

2.4. AFM

A Dimension ICON AFM (Bruker) was used to observe the morphology of the InP substrates. The AFM topography measurements were performed in air with the Peak Force tapping mode. For this purpose, a silicon tip on a nitride lever (ScanAsyst Air model, Bruker), with a 0.4 N/m spring constant and a nominal tip radius of 2 nm was used with a resolution of 256 pixels × 256 pixels.

3. Results and Discussion

3.1. Influence of the HCl concentration for (100) InP substrates

The immersion of (100) InP substrates within HCl solutions with different concentrations led to a large range of morphological evolutions as observed in Figure 1. Two different regimes can be distinguished: the low concentration range (from 0 to 6 M), where no gas emission was observed and the high concentration range (above 6 M), with a spontaneous and strong emission from all the InP surface in contact with the solution of an ultra-dense and characteristic fog of micro bubbles, due to the continuous release of PH_3.[19] Within the first regime, the integrity of the morphology is preserved (Figure 1 a. to f.) while surface degradation is noticeable in the second regime (Figure 1 g. to j.). According to the AFM images and the increase of the surface roughness, the degradation is evolving progressively with the HCl concentration, with the InP substrate immersed in the 9 M HCl solution representing the beginning of the degradation observed on the InP substrate immersed in the 12 M HCl. InP (100) substrates immersed in HCl 12 M showing a drastic topographic modification was already observed by Tuck and Baker,[20] but the progressivity of this morphological degradation at HCl concentrations higher than 6 M is shown here for the first time.

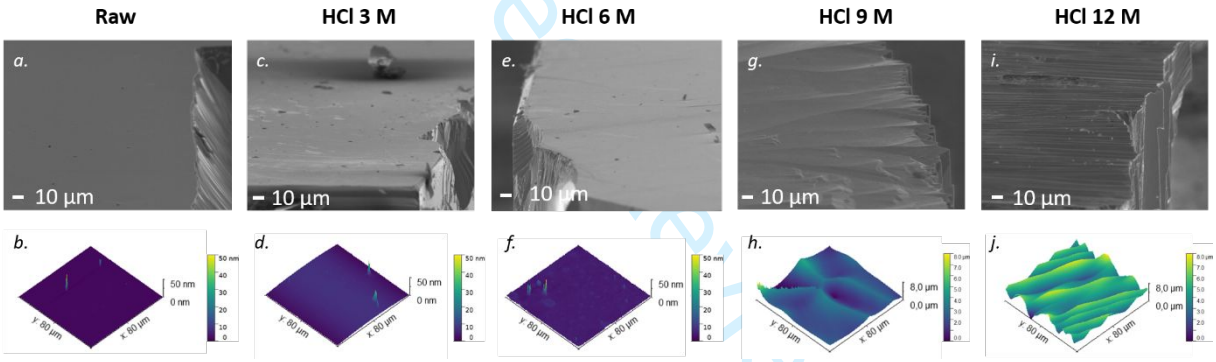

Figure 1: Cross-section SEM and AFM images for raw InP (100) substrate (a. and b.), InP (100) substrate immersed for 5 min in HCl 3M (c. and d.), InP (100) substrate immersed for 5 min in HCl 6M (e. and f.), InP (100) substrate immersed for 5 min in HCl 9 M (g. and h.) and InP (100) substrate immersed for 5 min in HCl 12 M (i. and j.).

As the morphological properties of the (100) InP substrate evolve with the HCl concentration, it is necessary to investigate also the potential modifications of the chemical properties, with XPS measurements. The In $3d_{5/2}$ and P 2p spectra are displayed in Figure 2 and the fit parameters are in Table 1. Regarding the raw (100) InP substrate (Figure 2 a. and b.) corresponding to the epiready configuration, two contributions are observed for the In $3d_{5/2}$ and the P $2p_{3/2}$ photopeaks: ones related to the InP substrate at 445.0 eV and 129.2 eV respectively, and the other ones related to the oxide phases, In-O contribution being at 445.9 eV and the P-O contribution being at 133.5 eV.[21] Quantitatively speaking, no specific enrichment in In or P is noticed on the surface of the raw (100) InP substrate, as expected for an epiready substrate.

As soon as the (100) InP substrate is immersed in HCl solution, the In-O contribution disappears while a small reminiscence (inferior to 0.6 at. %) of P-O is observed. No modification of the initial position of the photopeak is noticed and the modified Auger parameters remain in the associated range of the InP (852.6 eV).[21]

One could expect that the modification of the morphology would induce changes within the photopeak answer, with an enlargement of the full-width half at maximum (FWHM) for example.[22] However, as observed in Table 1, the FWHM values of the In $3d_{5/2}$ and P $2p_{3/2}$ photopeaks don't evolve, reaching 0.79 ± 0.01 eV and 0.60 ± 0.02 eV, respectively. The only noticeable difference is related to the phosphate contribution, with a larger range of value, which is attributed to the really low amount of oxide detected, inducing variabilities during the fitting procedure.

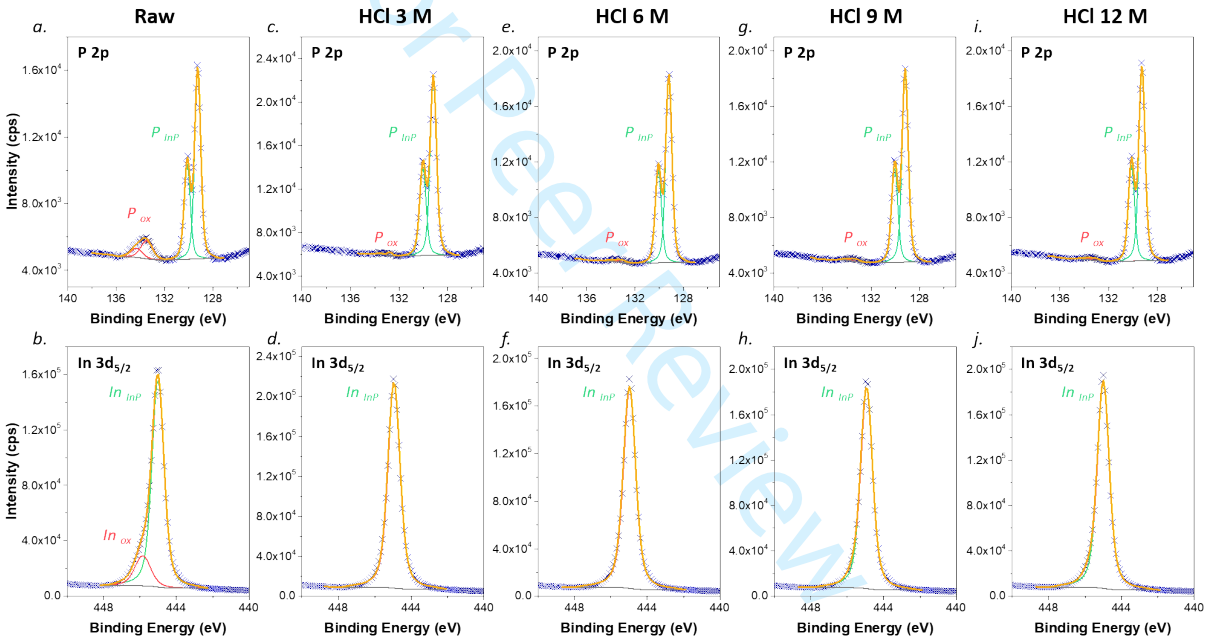

Figure 2: P 2p and In $3d_{5/2}$ XPS spectra for raw InP (100) substrate (a. and b.), InP (100) substrate immersed for 5 min in HCl 3M (c. and d.), InP (100) substrate immersed for 5 min in HCl 6M (e. and f.), InP (100) substrate immersed for 5 min in HCl 9 M (g. and h.) and InP (100) substrate immersed for 5 min in HCl 12 M (i. and j.).

Another expectation related to morphology evolution observed in Figure 1 could be an enrichment in In or P during the strong dissolution regimes (9 M and 12 M). The In/P ratios calculated in Table 1 refute this hypothesis since the In_{InP}/P_{InP} ratios remain within a range of 1.03 ± 0.05, the raw value being at 1.04. Thus, the surface chemistry of (100) InP substrate is not modified when exposed to a large range of concentrations of HCl, even if some morphological modifications appear.

Table 1: Parameters fits for the XPS spectra displayed in Figure 2. The ratios are calculated from the In $3d_{5/2}$ and P 2p photopeaks.

	Attribution	Position (eV)		FWHM (eV)		Ratios		Modified Auger parameter (eV)
		In $3d_{5/2}$	P $2p_{3/2}$	In $3d_{5/2}$	P $2p_{3/2}$	In_{InP} / P_{InP}	In_{tot} / P_{tot}	
Raw substrate	InP	445.0	129.2	0.79	0.59	1.04	1.05	852.7
	oxide	445.9	133.5	1.03	1.12			
HCl 3 M	InP	445.0	129.2	0.80	0.62	0.99	0.97	852.8
	oxide	/	132.9	/	0.90			
HCl 6 M	InP	445.0	129.2	0.78	0.60	1.04	1.02	852.7
	oxide	/	133.2	/	1.09			
HCl 9 M	InP	444.9	129.2	0.78	0.60	1.02	1.04	852.7
	oxide	/	133.3	/	0.94			
HCl 12 M	InP	445.0	129.2	0.79	0.60	1.04	1.06	852.7
	oxide	/	133.1	/	1.07			

3.2. Influence of the crystallographic orientation of the InP substrate

If the HCl concentration doesn't influence the chemical behaviour of (100) InP substrate, interrogations can remain about the influence of HCl when facing different crystallographic orientations of InP substrate. To elucidate it, (111) InP substrates, on face A (In-rich) and on face B (P-rich), as well as polycrystalline InP substrates, were immersed in HCl 12 M for 5 minutes.

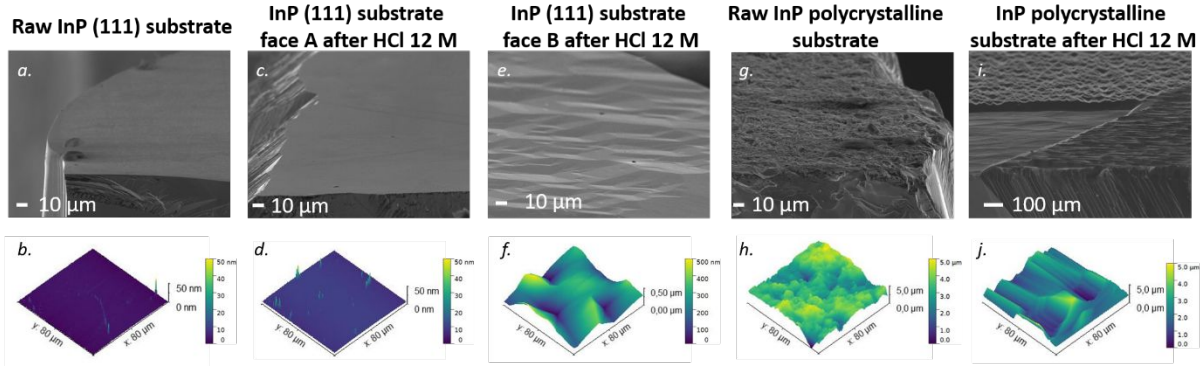

Figure 3: Cross-section SEM and AFM images for raw InP (111) substrate (a. and b.), InP (111) substrate face A (In-terminated) immersed for 5 min in HCl 12 M (c. and d.), InP (111) substrate

face B (P-terminated) immersed for 5 min in HCl 12 M (e. and f.), raw InP polycrystalline substrate (g. and h.) and InP polycrystalline substrate immersed for 5 min in HCl 12 M (i. and j.). Since faces A and B of the raw InP (111) substrate present similar surface aspect and rugosity, only one was represented here.

Regarding the (111) InP substrates, according the face observed, two different surface morphologies are obtained after the HCl treatment (Figure 3 a. to f.). One first face remains as smooth as the raw (111) substrate (whatever the face observed) when the other present a high rugosity. The difference between the two faces can be explained with the gas release. For the first face (Figure 3 c. and d.), only a small amount of PH_3 was released during the HCl immersion, while for the second face (Figure 3 e. and f.), an intense PH_3 release as important as the one observed for the (100) InP substrate is noticed, resulting in important modifications of the topography of the surface sample. Based on Tuck and Baker previous observations,[20] face 1 is thus the (111) A InP, terminated with an indium layer which tempers the release of PH_3 and face 2 is the (111) B InP, terminated with phosphorus atoms which immediately react with the acidic environment to release an important amount of PH_3.

Immersing the polycrystalline InP substrate into HCl doesn't result in a smoother surface (Figure 3 j.) but specific textures are observed, especially according to the initial grain orientations (Figure 3 i.). This difference of grain orientation induces also a difference of kinetics etching, as noticed with the specific step observed on Figure 3 i.

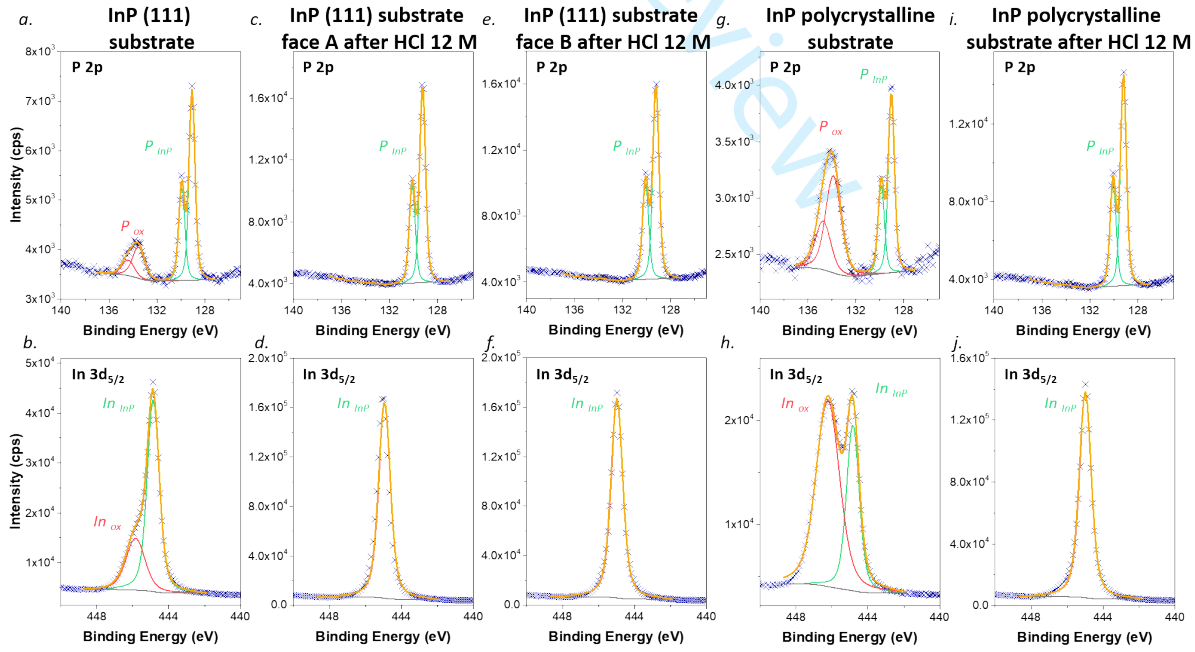

Figure 4: P 2p and In $3d_{5/2}$ XPS spectra for raw InP (111) substrate (a. and b.), InP (111) substrate face A (In-terminated) immersed for 5 min in HCl 12 M (c. and d.), InP (111) substrate face B (P-terminated) immersed for 5 min in HCl 12 M (e. and f.), raw InP polycrystalline

substrate (g. and h.) and InP polycrystalline substrate immersed for 5 min in HCl 12 M (i. and j.). Since faces A and B of the raw InP (111) substrate present similar fitting procedures, only one was represented here. Fit details are available in Table 2.

The chemical evolution of InP substrates is also studied according to the crystallinity evolution when the samples are immersed in HCl 12 M for 5 minutes (Figure 4 and Table 2). Whatever the crystallographic orientation, both raw substrates present important quantities of oxides, and, as soon as samples are immersed into HCl 12 M solution, the oxide contributions disappear, even the P-O one. This difference with the substrate (100) is explained with a shorter transfer time to the XPS analyses. Quantitatively speaking, the In_{InP}/ P_{InP} ratios of the polycrystalline and the (111) substrates are lower than the (100) raw substrate reference. This apparent modification is related to the important amount of oxide detected for the raw polycrystalline and the (111) InP substrates. In $3d_{5/2}$ and P $2p_{3/2}$ photopeaks are within an extended energy range, In $3d_{5/2}$ being at 445.0 ± 0.1 eV and P $2p_{3/2}$ at 129.2 ± 0.1 eV. Thus, the difference between the electron escape depths of these two photopeaks becomes too important, especially with the large oxide layers present at the substrates' surfaces. This difference can be overcome by choosing two photopeaks in a narrower energy range, such as In $4d_{5/2}$ (17.9 ± 0.1 eV) and P $2p_{3/2}$ (129.2 ± 0.1 eV). In this case, the In_{InP}/ P_{InP} ratios become 1.06 for the polycrystalline InP substrate and 0.92 for both (111) A and (111) B faces of InP (111) substrate.

Regarding the (111) substrates, after HCl immersion, similar fitting parameters and quantitative aspects are observed between the (100) InP substrate and the (111) face A. For the InP substrate (111) face B, a small enlargement of the P $2p_{3/2}$ contribution is noticed (Table 2), which was attributed to an additional contribution of the (111) face B surface of InP by Sturzenegger and Lewis (elementary phosphorus, responsible for the oxidation begin).[23] In the present case, it is not possible to confirm this additional contribution since the enlargement is quite small, but it is worth noticing it. A slight enrichment in In is also noticed for the (111) face B surface, confirming thus the morphological degradation observed, with a higher quantity of PH_3 released.

As expected,[22] the raw polycrystalline substrate presents slightly higher FWHM parameters, but the immersion in the concentrated HCl solution restore them within the range observed for (100) and (111) InP substrates. No specific enrichment in In or P is noticed, confirming thus what was observed with the (100) substrates: the dissolution in HCl solutions doesn't modify quantitatively the chemistry.

Table 2: Parameters fits for the XPS spectra displayed in Figure 4. The ratios are calculated from the In $3d_{5/2}$ and P 2p photopeaks.

	Attribution	Position (eV)		FWHM (eV)		Ratios		Modified Auger parameter (eV)
		In $3d_{5/2}$	P $2p_{3/2}$	In $3d_{5/2}$	P $2p_{3/2}$	In_{InP} / P_{InP}	In_{tot} / P_{tot}	
(111) face A raw substrate	InP	445.0	129.1	0.80	0.58	0.87	0.92	852.6
	Oxide	445.9	133.7	1.19	1.35			
(111) face B raw substrate	InP	444.9	129.1	0.79	0.59	0.80	0.86	852.7
	Oxide	445.8	133.6	1.23	1.20			
(111) face A HCl 12 M	InP	445.0	129.2	0.78	0.58	1.02	1.02	852.6
	Oxide	/	/	/	/			
(111) face B HCl 12 M	InP	445.0	129.2	0.78	0.61	1.08	1.08	852.7
	Oxide	/	/	/	/			
Polycrystalline raw substrate	InP	444.8	129.0	0.84	0.62	0.81	1.05	852.6
	Oxide	446.2	133.9	1.54	1.51			
Polycrystalline HCl 12 M	InP	445.0	129.2	0.80	0.59	1.04	1.04	852.6
	Oxide	/	/	/	/			

4. Conclusion

To understand the interactions between HCl solutions and InP surfaces during deoxidation and dissolution, the roles of the HCl concentration and the crystallographic orientation of the InP substrates were investigating. If a concentration frontier at 6 M is noticeable for the morphological evolution of the (100) InP substrates, with the destructuration of the InP network due to dissolution, no specific modification of the surface chemistry information is impacted by the concentration of HCl. Indeed, no enrichment in indium or phosphorus is observed, and this, within the first 10 nm of the substrate.

Regarding the crystallographic orientation, again, at high HCl concentrations, morphological modifications are noticed, with an important differentiation between the face A and the face B of the (111) InP substrate. However, those topographical evolutions don't influence the

chemical surface of the InP substrate, since the In_{InP}/P_{InP} ratios don't present any evolution even when facing HCl 12 M. Only a really small enrichment in In might be noticed in face B, with a more important quantity of P released during the dissolution of InP. Thus, it is possible to conclude that, whatever the crystallographic orientation of the InP substrates studied in this paper, the HCl concentration doesn't influence the chemical quantification of the InP substrate surface, even during strong dissolution of the substrates.

References

1. O'Leary SK, Foutz BE, Shur MS, Eastman LF. Steady-State and Transient Electron Transport Within the III–V Nitride Semiconductors, GaN, AlN, and InN: A Review. *J Mater Sci Mater Electron*. 2006;17(2):87-126. doi:10.1007/s10854-006-5624-2
2. LaPierre RR, Robson M, Azizur-Rahman KM, Kuyanov P. A review of III–V nanowire infrared photodetectors and sensors. *J Phys D Appl Phys*. 2017;50(12):123001. doi:10.1088/1361-6463/aa5ab3
3. Ekins-Daukes NJ. III-V Solar Cells. *Sol Cell Mater Dev Technol*. 2014;9780470065518:113-143. doi:10.1002/9781118695784.CH6
4. Thayne I, Hill R, Holland M, et al. Review of Current Status of III-V MOSFETs. *ECS Trans*. 2009;19(5):275-286. doi:10.1149/1.3119552/XML
5. Zavala-Moran U, Bouschet M, Perez JP, et al. Structural, Optical and Electrical Characterizations of Midwave Infrared Ga-Free Type-II InAs/InAsSb Superlattice Barrier Photodetector. *Photonics 2020, Vol 7, Page 76*. 2020;7(3):76. doi:10.3390/PHOTONICS7030076
6. Ren D, Farrell AC, Williams BS, Huffaker DL. Seeding layer assisted selective-area growth of As-rich InAsP nanowires on InP substrates. *Nanoscale*. 2017;9(24):8220-8228. doi:10.1039/C7NR00948H
7. Lau WM, Sodhi RNS, Ingrey S. Thermal desorption of oxides on InP. *Appl Phys Lett*. 1988;52(5):386. doi:10.1063/1.99474
8. Kaspari C, Pristovsek M, Richter W. Deoxidation of (001) III-V semiconductors in metal-organic vapour phase epitaxy. *J Appl Phys*. 2016;120:85701. doi:10.1063/1.4961414
9. Pahlke D, Kinsky J, Schultz C, et al. Structure of InP (001) surfaces prepared by decapping and by ion bombardment and annealing. *Phys Rev B*. 1997;56(4):R1661-R1663. doi:10.1103/PhysRevB.56.R1661
10. Losurdo M, Capezzuto P, Bruno G. Study of the H2 remote plasma cleaning of InP substrate for epitaxial growth. *J Vac Sci Technol B Microelectron Nanom Struct*. 1996;14(2):691. doi:10.1116/1.589158
11. Sun Y, Liu Z, MacHuca F, Pianetta P, Spicer WE. Optimized cleaning method for producing device quality InP(100) surfaces. *J Appl Phys*. 2005;97(12):0-7. doi:10.1063/1.1935745
12. Pluchery O, Chabal YJ, Opila RL. Wet chemical cleaning of InP surfaces investigated

by in situ and ex situ infrared spectroscopy. *J Appl Phys*. 2003;94(4):2707-2715. doi:10.1063/1.1596719

13. Notten PHL. The Etching of InP in HCl Solutions: A Chemical Mechanism. *J Electrochem Soc*. 1984;131(11):2641-2644. doi:10.1149/1.2115375/XML

14. Clawson A. Guide to references on III–V semiconductor chemical etching. *Mater Sci Eng R Reports*. 2001;31(1-6):1-438. doi:10.1016/S0927-796X(00)00027-9

15. Cuypers D, De Gendt S, Arnauts S, Paulussen K, van Dorp DH. Wet Chemical Etching of InP for Cleaning Applications . I. An Oxide Formation/Oxide Dissolution Model. *ECS J Solid State Sci Technol*. 2013;2(4):P185-P189. doi:10.1149/2.020304jss

16. van Dorp DH, Cuypers D, Arnauts S, Moussa A, Rodriguez L, De Gendt S. Wet Chemical Etching of InP for Cleaning Applications. II. Oxide Removal. *ECS J Solid State Sci Technol*. 2013;2(4):P190-P194. doi:10.1149/2.025304jss

17. Aytac S, Schlachetzki A, Prehn H-J. Thinning of InP by chemical etching. *J Mater Sci Lett*. 1983;2(8):447-450. doi:10.1007/BF00723690

18. Cuypers D, van Dorp DH, Tallarida M, et al. Study of InP Surfaces after Wet Chemical Treatments. *ECS J Solid State Sci Technol*. 2014;3(1):N3016-N3022. doi:10.1149/2.005401jss

19. Kafalas JA, Gatos HC, Button MJ. Hydrolysis of A III B V Intermetallic Compounds. *J Am Chem Soc*. 1957;79(16):4260-4261. doi:10.1021/ja01573a004

20. Tuck B, Baker AJ. Chemical etching of {1 1 1} and {1 0 0} surfaces of InP. *J Mater Sci*. 1973;8(11):1559-1566. doi:10.1007/BF00754890

21. Naumkin A V., Kraut-Vass A, Gaarenstroom SW, Powell CJ. NIST X-ray Photoelectron Spectroscopy Database. doi:10.18434/T4T88K

22. Béchu S, Loubat A, Bouttemy M, Vigneron J, Gentner J-L, Etcheberry A. A challenge for x-ray photoelectron spectroscopy characterization of Cu(In,Ga)Se2 absorbers: The accurate quantification of Ga/(Ga + In) ratio. *Thin Solid Films*. 2019;669:425-429. doi:10.1016/J.TSF.2018.11.029

23. Sturzenegger M, Lewis NS. An X-Ray Photoelectron Spectroscopic and Chemical Reactivity Study of Routes to Functionalization of Etched InP Surfaces. *J Am Chem Soc*. 1996;118(12):3045-3046. doi:10.1021/ja9536911